Morphology of Methane and Carbon Dioxide Hydrates Formed from Water Droplets

Phillip Servio and Peter Englezos
Dept. of Chemical and Biological Engineering, University of British Columbia, Vancouver, BC, Canada V6T 1Z4

Methane and carbon dioxide hydrate crystals were formed on nearly spherical water droplets at 274.6 K and 2,150 kPa or 1,000 kPa above the corresponding three-phase hydrate equilibrium pressure. Each experiment was performed with two droplets 5 mm and 2.5 mm in diameter or three droplets with a diameter of 2.5 mm. At the higher pressure the water droplets quickly became jagged and exhibited many needlelike or hairlike crystals extruding from the droplet, whereas at the lower pressure the surface was smooth. In almost all experiments, a depression or collapse of the hydrate layer was observed to occur. This collapse was interpreted as evidence of a continuing hydrate formation after the droplet surface was covered by the hydrate layer. The type of hydrate-forming gas and the size of the droplet was observed not to influence the macroscopic hydrate crystal morphology. The decomposition of the methane and carbon dioxide hydrate layers was also observed. Reformation was also experimented, and the effect of memory on the morphology of hydrate crystal growth was determined.

Introduction

Carbon dioxide and methane are known to form structure I hydrate crystals (Sloan, 1998). Methane gas hydrate occurs naturally in the earth (Sloan, 1998). According to Suess et al. (1999), the amount of organic carbon entrapped in hydrate exceeds all other reserves (fossil fuels, soil, peat, and living organisms). This hydrate is considered a future energy source and a potential global climate hazard (Englezos, 1993, 2001). Carbon dioxide and water are often found together in natural gas streams and in oil reservoirs and may form hydrate under proper thermodynamic and material availability conditions. CO_2 is a greenhouse gas and the option of sequestering it in the deep ocean is being explored (Brewer et al., 1999). Under favorable conditions this sequestered CO_2 may form hydrates. Finally, another technology involving hydrates is natural gas storage and transportation in the hydrate state (Khokhar et al., 2000).

Crystal morphology studies give valuable information on the mechanistic aspects of hydrate crystal nucleation, growth, and decomposition. Makogon reported a variety of hydrate crystals including threadlike and dendritic (Makogon, 1997). The various geometries were attributed to factors such as the variation in hydrate-forming gas, the supercooling, and the pressure. Maini and Bishnoi (1981) and Topham (1984) observed hydrate formation on methane bubbles or natural gas released in a downflow of seawater in a simulated deep-sea environment. It was observed that hydrates formed on the bubble and grew until the bubble was entrapped in a hydrate layer.

Mori's group studied liquid fluorocarbons (CFC-12, HFC-134a) that form hydrates in the presence of water (Mori and Mori, 1989a,b; Isobe and Mori, 1992). In their experiments, the liquid fluorocarbon was injected continuously into a pool of water. Formation of hydrates on the surface of the fluorocarbon was observed. Nojima and Mori (1994) studied CFC-11 and HFC-141b hydrate formation. In these experiments one bubble of fluorocarbon was held virtually stationary in a downflow of water. It was found that the hydrate first appeared on the surface of each bubble in the form of tiny particles that were swept to the back of the bubble and accumulated until a hydrate layer surrounded the entire bubble.

Sugaya and Mori (1996) carried out morphological studies using HFC-134a in the vapor or liquid state and water. It was found that the degree of supersaturation of the water with the fluorocarbon strongly influences the surface morphology

Correspondence concerning this article should be addressed to P. Englezos.

of the formed hydrate layer. It was found that the hydrate layer formed on the surface of a fluorocarbon drop held stationary is not as porous as the coagulated hydrate particles observed on the surface of buoying fluorocarbon bubbles (Nojima and Mori, 1994). Sugaya and Mori (1996) also referred to work by Aya et al. (1993) and Shindo et al. (1993), who placed CO_2 drops on a solid plate and a wire grid, respectively, immersed in quiescent water or seawater not saturated with CO_2. These experiments were performed at 30 MPa, which corresponds to a depth of 3 km in the sea. Immediate formation of a thin, smooth, semitransparent hydrate film on the surface of each drop was observed in both studies.

Uchida et al. (1999) studied the behavior of water droplets (several millimeters in diameter) in liquid CO_2. They observed the formation of a hydrate film at the water–CO_2 interface. It was suggested that the film grows primarily in the water phase. Kobayashi et al. (2001) also studied a hydrate film that was formed at the water–liquid HCFC-141b interface. Whether it was or was not exposed to flowing water was found to influence the morphology of the film.

Ohmura et al. (1999) carried out experiments with pure or presaturated water that was in contact with R-141b. It was found that presaturated water at high subcooling ($\sim$ 6.5 K) exhibited two stages of hydrate-crystal growth with different morphology. Kato et al. (2000) investigated the drop-formation behavior of HCFC-141b at a single nozzle in a water stream. It was observed that two discrete hydrate crusts grew along the liquid–liquid interface. Morphological observations of the decomposition of CO_2 hydrate into CO_2 gas or liquid were carried out by Uchida et al. (2000). The hydrate was first formed at the interface between water and liquid CO_2. It was found that decomposition from the increased temperature was more rapid due to the release of CO_2 gas that mechanically broke the hydrate. A decrease in pressure also evolved CO_2, which in turn mechanically broke the hydrate. Hydrate reformation indicated that the CO_2 concentration remaining in the solution after one growth and decomposition cycle affected reformation, giving either a film or a dendritic crystal.

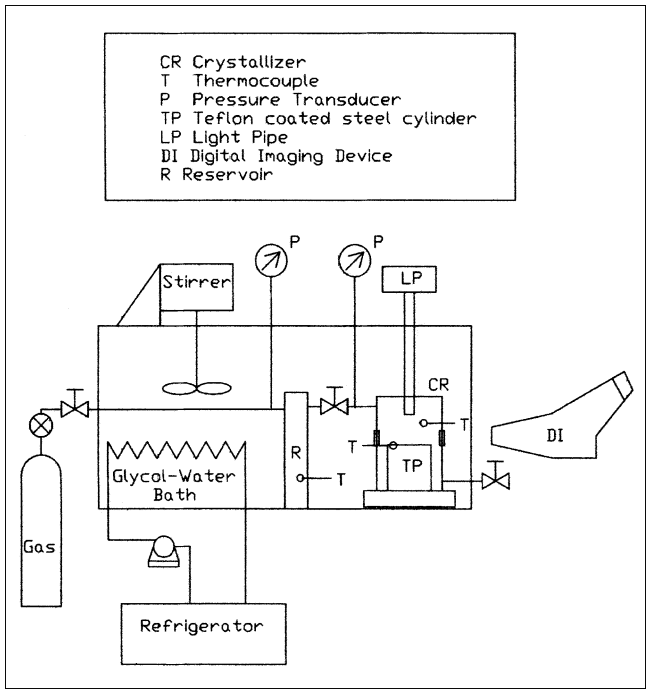

Figure 1. Simplified experimental apparatus.

Fukumoto et al. (2001) studied the hydrate formation on water sprayed into a HFC-32 gas chamber. A nozzle was used to direct water at a copper-block surface. It was observed that coating the copper-block surface with a thin layer of supercooled water or ice would immediately induce hydrate formation. Furthermore, when the water was sprayed upwards from a hollow-cone nozzle, then a wet hydrate deposit that grew into the form of a veil or a skirt was observed.

As seen, morphological studies reveal important information about the mechanistic aspects of hydrates. This information has aided modeling efforts (Mochizuki and Mori, 2000; Mori and Mochizuki, 2000). Most of the experimental studies on crystal morphology have been focused on CO_2 droplets or CH_4 bubbles or fluorocarbons in the liquid or vapor phase in the presence of water as the bulk phase. Moreover, crystal morphology experiments in the past have been limited to monitoring one droplet at a time. The objective of this study is to conduct crystal morphology experiments with two or three stagnant water droplets simultaneously. The hydrate-forming gas, CH_4 or CO_2, constitutes the bulk phase. Thus, the work is relevant to technology development for natural gas storage/transport in hydrate form and carbon dioxide sequestration.

Experimental Apparatus and Procedure

The apparatus consisted of a stainless-steel hydrate crystallizer submerged in a bath that contained a 50-50 wt% mixture of water and ethylene glycol. A simplified experimental apparatus is given in Figure 1. Details of the apparatus are given elsewhere (Servio, 2002). The crystallizer has three windows, one on the top made from Plexiglas (polymethyl methacrylate) and two on the sides made out of Lexan (polycarbonate). The Lexan windows positioned on the sides of the hydrate crystallizer are used for viewing, while the Plexiglas window mounted on the top of the reactor is fitted for a fiber-optic light pipe that can deliver 40,000 foot-candles of light. The fiber-optic light pipe (41720 series, Cole Palmer, Anjou, P. Q., Canada) is equipped with an infrared filter to minimize or eliminate heat transmission. The digital imaging is carried out by a Nikon SMZ 2000 microscope fitted with a 3.34 mega pixel Nikon CoolPix 995 digital camera. The output of the camera is also viewed and recorded by a PC through a Dazzle digital video creator.

The droplets are placed on a 316 stainless-steel cylinder covered with a layer of Teflon to prevent the water droplets from wetting the surface. Two copper–constantan thermocouples are used to report the temperature in the crystallizer to 0.1 K. One thermocouple is positioned at the surface of the Teflon to measure the surface temperature and one is positioned solely in the gas phase. The pressure in the crystallizer is measured by a Rosemount Smart Pressure transducer (3051CD, Norpac Controls, Vancouver, B.C., Canada) with a range of 0–13,790 kPa and an accuracy of 0.075% of the span.

The procedure involves cleaning and drying the inside of the hydrate crystallizer as well as the stainless-steel cylinder and Teflon on which the droplets reside. The droplets are made from distilled and deionized water and are placed on the Teflon-coated cylinder with the aid of a Hamilton microsyringe. The reactor is then closed and flashed three times, with the hydrate-forming gas at 1,000 kPa to remove any residual gas still present in the reactor. The hydrate-forming gas (UHP CH_4 or UHP CO_2) is then fed into the reactor from a supply reservoir, which is at the experimental temperature.

Extensive trials were conducted to choose the best lighting position that would extract the most amount of detail from the crystal formation. It was found that lighting from the back of the reactor made it extremely difficult to view needle formation extending away from the droplets as well as any deviations in the surface sphericity. The lighting assignment that gave the best results was from directly above and that was followed in the experiments presented in this work.

Hydrate formation

The hydrate-formation experiments were performed at 274.6 K and under two different pressures to observe the effect of the driving force. The two experimental pressures were 2,150 kPa (high driving-force conditions) and 1,000 kPa (low driving-force conditions) above the three-phase equilibrium for methane and carbon dioxide, respectively. The three-phase equilibrium pressure at 274.6 K is 1,386 kPa for carbon dioxide hydrate and 2,900 kPa for methane hydrate, respectively (Sloan, 1998).

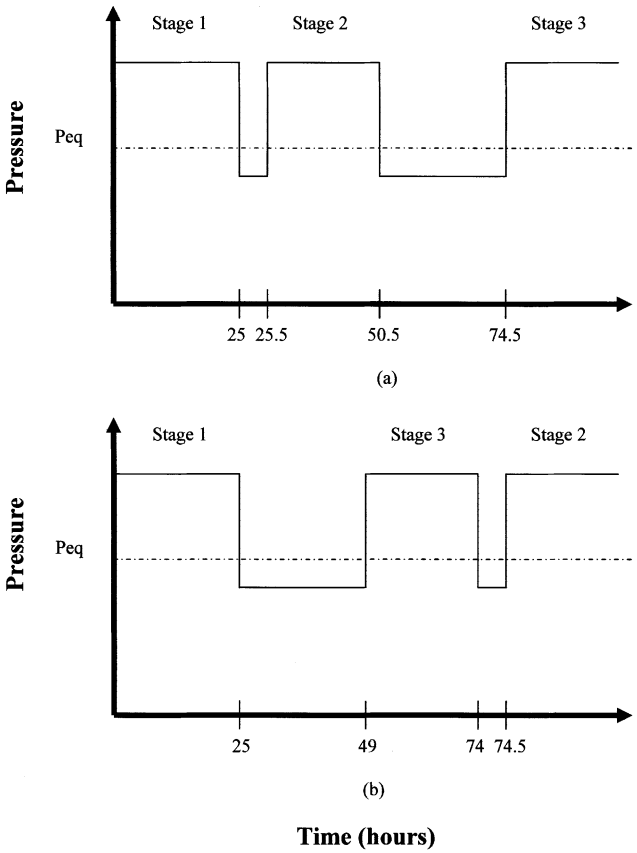

Figure 2. Pressure variation in a reformation experiment vs. time for sequences (a) and (b).

Peq is the three-phase equilibrium pressure.

Hydrate decomposition

The procedure for hydrate decomposition was to reduce the pressure to a value 10% below the three-phase equilibrium pressure. The pressure was reduced approximately 100 kPa/min until the desired experimental pressure was obtained. Once the pressure was stable, the morphological changes vs. time were recorded.

Hydrate reformation

The reformation experiments were performed in three stages. During the first stage hydrates were formed at 274.6 K and 5,100 kPa for methane or 3,540 kPa for carbon dioxide. These hydrate crystals were allowed to grow for 25 h. After 25 h the hydrate crystals were decomposed in the same manner as a decomposition experiment. In stage 2 the hydrates were maintained at the decomposition pressure for 30 min before restoring the pressure back to stage 1 conditions. The hydrates were then formed and allowed to grow for a period of 25 h before decomposing once again. During stage 3 the pressure was maintained at the decomposition pressure for 24 h before increasing it back into the hydrate-formation region. Stages 2 and 3 were performed once in the sequence just described (sequence a) and once in the reverse order, stage 3 before stage 2 (sequence b), for both methane and carbon dioxide. Figure 2 shows the variation in pressure with time for both sequences.

Results and Discussion

The first sets of experiments (1 to 3 and 10 to 12 in Table 1) were performed under a high driving force. The average induction time was 18 min for CO_2 and 67 min for CH_4. The difference can be attributed to the fact that CO_2 is much more soluble in water than CH_4. Solubility data for CH_4 and

Table 1. Experimental Conditions Along with Measured Induction Times

Exp.	No. of Droplets	Gas	Droplet Size (mm)	*P* (kPa)	Induct. Time (min)
1	3	CO_2	2.5	3,540	13
2	3	CO_2	2.5	3,540	24
3	3	CO_2	2.5	3,540	17
4	2	CO_2	5 & 2.5	3,540	39
5	2	CO_2	5 & 2.5	3,540	14
6	2	CO_2	5 &2.5	3,540	21
7	2	CO_2	5 &2.5	2,390	*
8	2	CO_2	5 & 2.5	2,390	478
9	2	CO_2	5 & 2.5	2,390	562
10	3	CH_4	2.5	5,100	85
11	3	CH_4	2.5	5,100	79
12	3	CH_4	2.5	5,100	37
13	2	CH_4	5 & 2.5	5,100	60
14	2	CH_4	5 & 2.5	5,100	44
15	2	CH_4	5 & 2.5	5,100	29
16	2	CH_4	5 & 2.5	3,950	*
17	2	CH_4	5 & 2.5	3,950	587
18	2	CH_4	5&2.5	3,950	*

*Did not nucleate within 5 days.

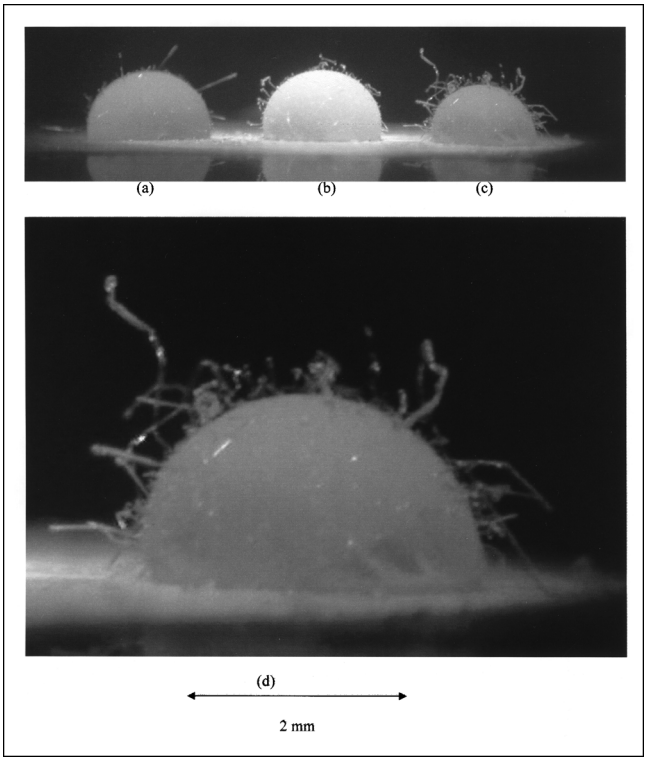

Figure 3. Methane hydrate covering the surface of water droplets (a,b,c) under high driving force, 10 min after nucleation (exp. 10).

Picture (d) is a magnified view of droplet (c).

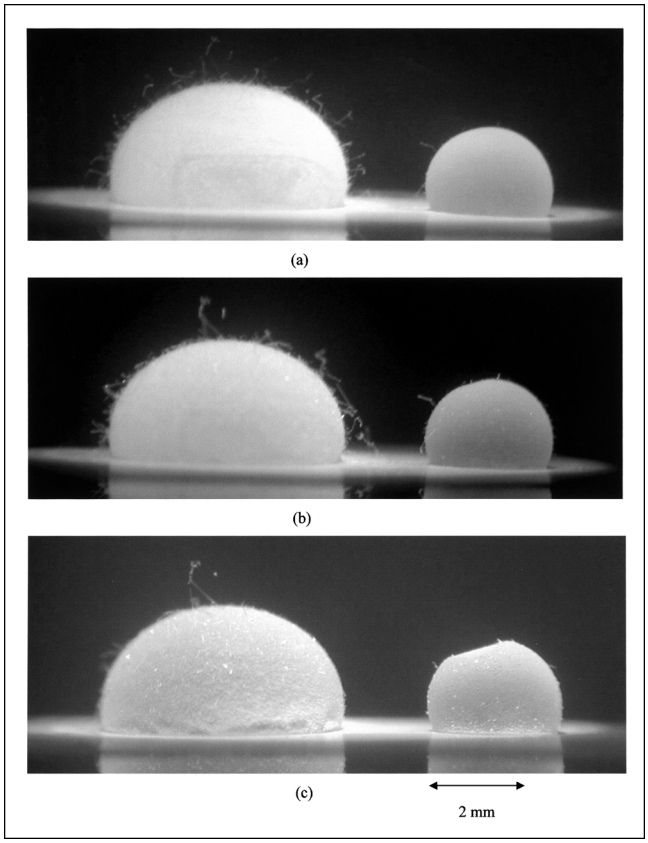

Figure 4. Carbon dioxide hydrate covering two water droplets under high driving force at three different times after nucleation (exp. 4): (a) 1 h; (b) 5 h; (c) 20 h.

CO_2 in water in the presence or absence of the corresponding hydrate are given by Servio and Englezos (2001, 2002). It was observed that in each of these experiments the three droplets nucleated simultaneously. This phenomenon might be random, but the possibility that it is due to external factors is not excluded. One possibility is the existence of numerous microscopic water droplets on the Teflon surface that create a "bridge" between the three droplets. When these droplets nucleate, the information is transmitted to the three droplets, and, thus, they nucleate at the same time. The existence of the microscopic droplets can be attributed to water condensing on the Teflon-coated surface. Minute temperature differences inside the crystallizer due to the illumination from the fiber-optic light or the low thermal conductivity of gas inside the crystallizer could make the surface of the stainless-steel cylinder colder than the water droplet surface. This could lead to the evaporation of water on the water droplet surface, followed by condensation on the Teflon surface.

It was observed that within less than 5 s after nucleation the surface of the droplet quickly became jagged and exhibited many fine needle-like crystals extruding away for the gas–hydrate–water interface, as seen in Figure 3. This was true for all cases observed under high driving force, independent of the hydrate-forming gas. It can also be seen from Figure 3 that the thickness and length of the hydrate needles extruding from the surface is related to the size of the droplet. Droplet 3c was initially the same size as droplets 3a and 3b. It decreased in size significantly with respect to the first two droplets. This is apparently because of the larger amount of water that participated in forming the network of crystals extending away for the hydrate-gas interface.

During the next sets of experiments (4 to 9 and 13 to 18 in Table 1) a better understanding of the effect of driving force and droplet size on the macroscopic crystal morphology was obtained. Once again, it was found that both droplets nucleated at approximately the same time in experiments under high and low driving force. Furthermore, the hydrate formation under high driving force was observed to evolve in phases. During the first phase, a hydrate layer appeared around the water droplet along with the needle-like crystals, as seen in Figure 4. After a period of time, up to 10 h after nucleation, the needle-like crystals grew in size and thickness. The second phase began with the collapse of most of the crystal needles onto the hydrate layer covering the water droplet. The last phase was the appearance of depressions in the hydrate layer surrounding the water droplet. It should be noted that the appearance of the third phase could take 10–15 hours to a couple of days in some cases. The collapse of the hydrate layer surrounding the droplets is considered evidence that water is still being converted to hydrate, even after the formation of a hydrate layer. It is noted that this collapse was also observed in experiments 1 to 3 and 10 to 12.

Experiments under low driving force conditions in which hydrates did not form within five days were terminated. How-

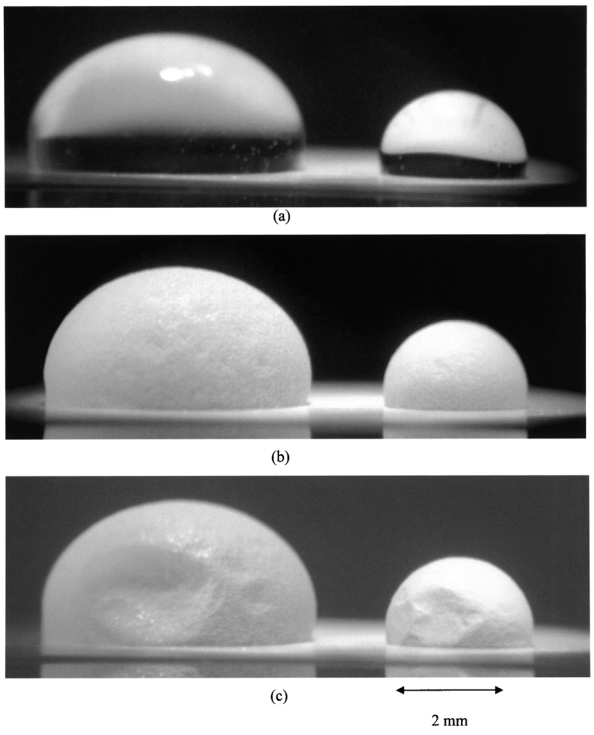

Figure 5. Methane hydrate covering two water droplets under low driving force at three different times (exp. 17): (a) water droplets at the beginning of experiment; (b) hydrate covered water droplet 10 h after experiment began; (c) hydrate covered water droplet 25 h after experiment began.

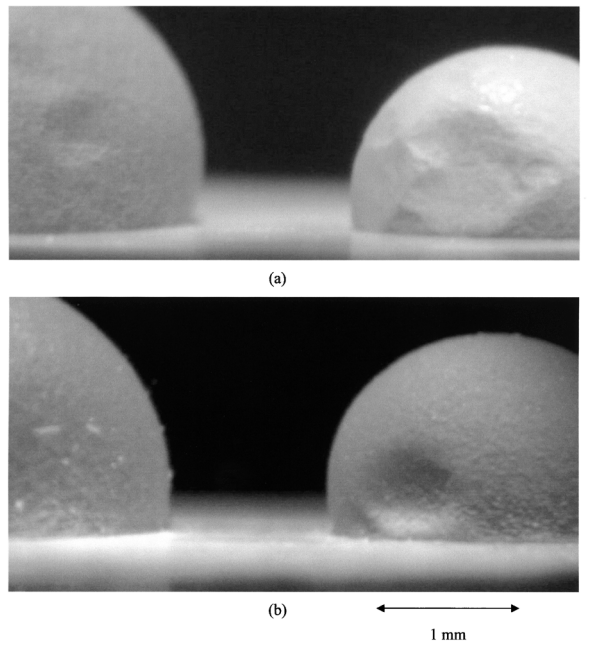

Figure 6. Methane hydrate surfaces from water droplets after 25 h of hydrate growth (exp. 17 & 14): (a) low driving force; (b) high driving force.

ever, one experiment for methane and two for carbon dioxide formed hydrates as seen in Table 1 (experiments 8, 9, and 17). The first observation during the low-pressure experiments was the absence of any hydrate needles from the hydrate-covered droplet. The texture was smooth and shiny, as seen in Figure 5. Figure 6 shows a comparison of the surface morphology obtained under a high driving force (rough and dull), and with that obtained under a low driving force (smooth and shiny).

The difference in surface roughness and the appearance of hydrate needles can be postulated to depend on the density of hydrate nuclei formed, which in turn depends on the magnitude of the driving force. Under the high driving force nucleation occurs at a larger number of sites on the droplet surface compared to the number of sites under low driving force. The rate of nucleation (amount of nuclei formed per unit time per unit volume) increases with the degree of supersaturation (Mullin, 1997). The degree of supersaturation is proportional to the driving force. Thus, hydrate nucleation under the higher driving force gives rise to many crystal growth centers with faster nucleation kinetics. It is postulated that this gives rise to more random crystal growth, leading to a rough surface. Under low driving force conditions, nucleation occurs at a decreased number of sites, compared to the higher driving force. Growth occurs preferentially at these sites, and since more free water on the surface of the droplet is available growth occurs across the droplet surface until it is covered with a smooth layer of hydrate.

The actual mechanism of hydrate growth on the water droplets is not known, but it may be assumed that water is transferred through capillaries within the porous hydrate layer and reacts with gas that is surrounding the droplet. It is noted that water permeation through the hydrate film was also reported by Sugaya and Mori (1996) and Kobayashi et al. (2001). It is also noted that gas can diffuse through the hydrate layer and "react" with water (Hatzikiriakos and Englezos, 1994). However, it is difficult to establish how significant this is for hydrate growth.

It is interesting to note that Ohmura et al. (1999) and Uchida et al. (1999) also observed the appearance of crystals growing radially around their hydrate-covered surface. Ohmura et al. (1999) described these crystals as platelike and standing upright on the outer surface of the drop-enclosing hydrate shell formed. Ohmura et al. (1999) also noted that the platelike crystals were never observed in the presence of pure water and/or small subcooling (~ 2 K). This result is consistent with our findings of needle-like crystals extruding radially from the surface of our hydrate-covered droplets under high driving force. There are two significant differences between the findings of Ohmura et al. (1999) and Uchida et al. (1999) and this current study. First is that the hydrate needles in this work extrude into the hydrate-formation (CH_4 or CO_2) phase, while hydrate plates in the experiments of Ohmura et al. (1999) and Uchida et al. (1999) extruded into the water phase. Second, the hydrate needles grew almost

Table 2. Experimental Conditions for Reforming Hydrate Crystals on Two Water Droplets of Previously Formed Hydrates

Exp.	Stage	Gas	Droplet Size (mm)	P (kPa)	Induct. Time (min)
	1st Formation	CH_4	5 & 2.5	5,100	310
1a	2nd Formation *	CH_4	5 & 2.5	5,100	7
	3rd Formation**	CH_4	5 & 2.5	5,100	187
	1st Formation	CH_4	5 & 2.5	5,100	167
1b	2nd Formation**	CH_4	5 & 2.5	5,100	57
	3rd Formation*	CH_4	5 & 2.5	5,100	2
	1st Formation	CO_2	5 & 2.5	3,540	112
2a	2nd Formation*	CO_2	5 & 2.5	3,540	3
	3rd Formation **	CO_2	5 & 2.5	3,540	35
	1st Formation	CO_2	5&2.5	3,540	67
2b	2nd Formation **	CO_2	5 & 2.5	3,540	49
	3rd Formation *	CO_2	5&2.5	3,540	4

Note: Measured induction times are also given.
* Reformation of hydrates after being allowed to decompose for 30 min.
** Reformation of hydrates after being allowed to decompose for 24 h.

simultaneously with the lateral growth of a hydrate film along the droplet surface in this study. On the other hand, the formation of platelike crystals appeared much later than the hydrate film in the work of Ohmura et al. (1999) and Uchida et al. (1999).

Four hydrate re-formation experiments were carried out to investigate the effect of memory on the water droplets. Memory refers to water having experienced hydrate formation/decomposition. Details of the experimental conditions are given in Table 2. First, it is noted that the average induction time for the first methane hydrate formation (no memory) was 248.5 min ((310 + 167)/2), whereas for carbon dioxide hydrate it was 89.5 min ((112 + 67)/2). As expected, the induction time for CO_2 hydrate is shorter. However, these induction times for CO_2 and CH_4 hydrate are much longer than the corresponding times from Table 1. In particular the average induction time from experiments 13 to 15 is 44.3 min for methane hydrate and 24.7 min for carbon dioxide hydrate from experiments 4 to 6. As expected, the induction time for CO_2 is shorter than for CH_4. However, the fact that there is a difference between the induction times for the same gas in Tables 1 and 2 illustrates the well-known facts that the induction time for hydrate nucleation has a random component, it is system dependent, and it is very difficult to establish perfect homogeneous nucleation conditions (Englezos, 1996; Sloan, 1998).

In spite of the different induction times, the morphology of the growing crystal was found to be independent of the induction time but dependent on the magnitude of the driving force. In particular, it was observed that if the hydrates were allowed to decompose for at least 24 h before reformation, then the surface would become rough and jagged with many needle-like crystals extending radially away from the surface, as seen in Figure 7b. The appearance of the hydrate surface in Figure 7b is similar to that obtained with hydrate nucleation under high driving force using water droplets with no memory of hydrate formation (Figures 3, 4, and 6b). Figure 7a shows the state of the hydrate-covered drop before decomposition for 24 h. This hydrate surface is slightly jagged due to the collapse of its hydrate needles and exhibits surface depressions due to water depletion. When the hydrate crystals were decomposed for 30 min and hydrates later formed using the same water droplet, the nucleation was instantaneous. In that case, the hydrate-covered droplets seen in Figure 7c exhibited the same morphology as hydrate crystals that had nucleated under low driving force conditions (Figures 5 and 6a). Nucleation after 30 min of decomposition occurs on water that most likely has hydrate templates, and, hence, a smaller number of nuclei is obtained. It is noted that memory effects were also reported by Uchida et al. (2000).

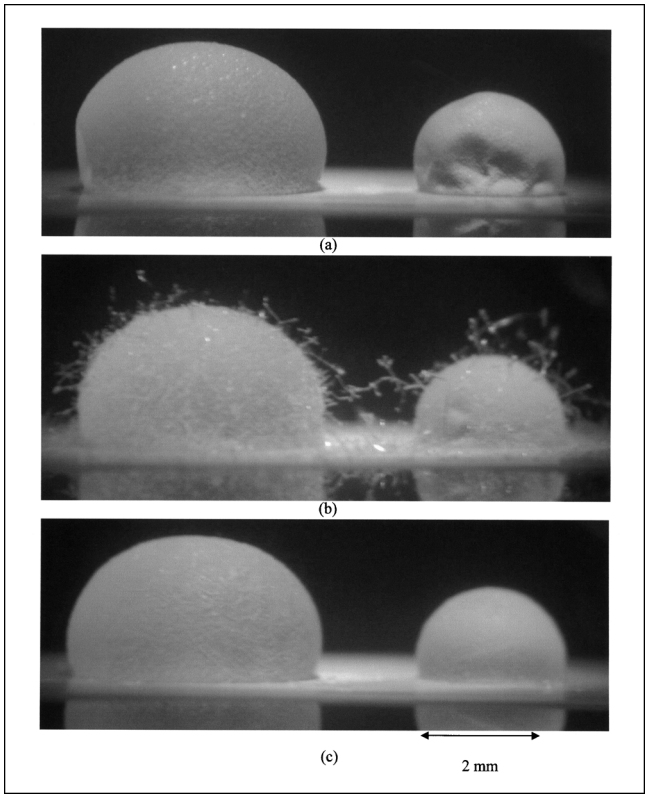

Figure 7. Carbon dioxide hydrate formation from water droplets (exp. 2b) (a) hydrate growth for 25 h on water with no previous hydrate memory; (b) 10 min of hydrate growth after being decomposed for 24 h prior; (c) 10 min of hydrate growth after being decomposed for 30 min prior.

Finally, experiments were performed to observe the decomposition of hydrates that had previously formed on the water droplets. It was found that the decomposition was macroscopically the same for high as for low driving force, and was independent of the hydrate-forming gas. Hydrates disappeared from macroscopic view approximately 30 minutes after the pressure decrease. Figure 8 shows two water droplets covered by hydrates as they decomposed. The growth of the hydrate droplet shown in Figure 8 was presented in Figure 4. The hydrate surface looks almost liquid-like or gel-like after five minutes of dissociation. Five to 15 min later the gas–liquid surface was visible as were crystals, which are con-

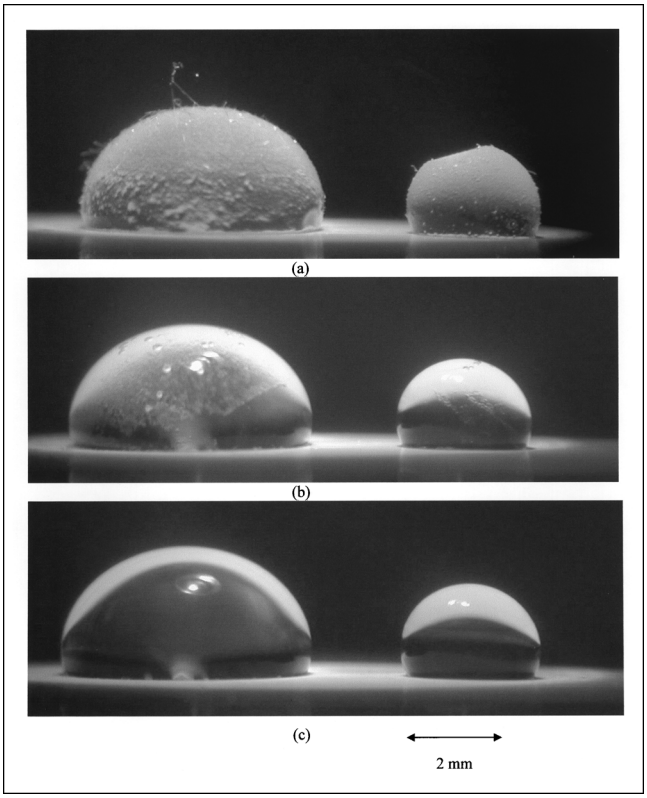

Figure 8. Decomposition of carbon dioxide hydrates formed under high driving force (exp. 4) after its beginning: (a) 5 min; (b) 20 min; (c) 30 min.

sidered to be hydrate sheets. As seen in Figure 9, these hydrate sheets were thin and transparent. It was also observed that they migrated to the top of each droplet until they vanished. Gas bubbles were also seen rising to the top of the droplets.

Conclusions

Macroscopic crystal morphology observations were made on methane and carbon dioxide hydrates formed on water droplets at 274.6 K and 2,150 kPa or 1,000 kPa above the corresponding three-phase equilibrium pressure. Each experiment was performed with two droplets 5 mm and 2.5 mm in diameter, or three droplets with a diameter of 2.5 mm. It was found that all droplets in a given experiment nucleated simultaneously. The size of the droplet had no noticeable effect on nucleation time or macroscopic crystal morphology. On the other hand, the driving force affected the crystal morphology greatly. Under high driving force crystals nucleated much sooner, the surface was slightly jagged, and numerous needle-like crystals extended away from the hydrate–gas interface. Under low driving force, needle-like crystals were not present, and the surface was smooth and shiny. In all experiments it was observed that the type of hydrate-forming gas did not have any effect on the crystal morphology. Hydrate-formation experiments using water droplets that had undergone hydrate formation and decomposition revealed that the time that the droplet remained in the decomposed state influenced the morphology of the crystal obtained. Finally, independent of the initial driving force or hydrate-forming gas, the hydrate crystals decomposed in much the same manner.

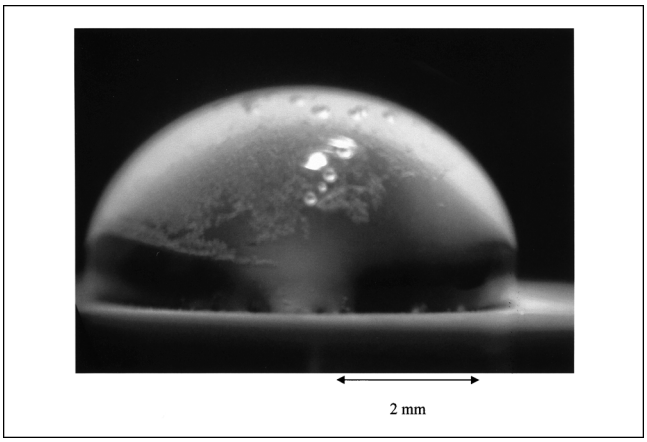

Figure 9. Closeup of the droplet on the left side of Figure 8b.

Acknowledgments

Financial support from the Natural Sciences and Engineering Research Council of Canada (NSERC) and The Institute of Applied Energy (IAE), Japan, is greatly appreciated.

Literature Cited

Aya, I., K. Yamane, and N. Yamada, "Stability of Clathrate-Hydrate of Carbon Dioxide in Highly Pressurized Water (in Japanese)," *Trans. JSME*, **59b**, 1210 (1993).

Brewer, P. G., C. Friederich, E. T. Peltzer, and F. M. Orr, Jr., "Direct Experiments on the Ocean Disposal of Fossil Fuel CO_2," *Science*, **284**, 943 (1999).

Englezos, P., *Energy, Environment, and Naturally Occurring Methane Gas Hydrate: Connections, in Energy and Environment: Technological Challenges for the Future,* Y. H. Mori and K. Ohnishi, eds., Springer-Verlag, Tokyo, p. 181 (2001).

Englezos, P., "Clathrate Hydrates," *Ind. Eng. Chem. Res.*, **32**, 1251 (1993).

Englezos, P., "Nucleation and Growth of Gas Hydrate Crystals in Relation to Kinetic Inhibition," *Rev. Inst. Fr Pet.*, **51**, 789 (1996).

Fukumoto, K., J. Tobe, R. Ohmura, and Y. H. Mori, "Hydrate Formation Using Water Spraying in a Hydrophobic Gas: a Preliminary Study," *AIChE J.*, **47**, 1899 (2001).

Hatzikiriakos, S. G., and P. Englezos, "Gas Storage Through Impermeation of Porous Media by Hydrate Formation," *Proc. Int. Offshore and Polar Engineering Conf.*, J. S. Chung, B. J. Natvig, and B. M. Das, eds., Osaka, Japan, p. 337 (1994).

Isobe, F., and Y. H. Mori, "Formation of Gas Hydrate or Ice by Direct-Contact Evaporation of CFC Alternatives," *Int. J. Refrig.*, **15**, 137 (1992).

Kato, M., T. Iida, and Y. H. Mori, "Drop Formation Behaviour of a Hydrate-Forming Liquid in a Water Stream," *J. Fluid Mech.*, **414**, 367 (2000).

Khokhar, A. A., E. D. Sloan, and J. S. Gudmundsson, "Natural Gas Storage Properties of Structure H hydrate," *Ann. N.Y. Acad. Sci.*, **912**, 950 (2000).

Kobayashi, I., Y. Ito, and Y. H. Mori, "Microscopic Observations of Clathrate-Hydrate Films Formed at Liquid/Liquid Interfaces. I. Morphology of Hydrate Films," *Chem. Eng. Sci.*, **56**, 4331 (2001).

Maini, B. B., and P. R. Bishnoi, "Experimental Investigation of Hydrate Formation Behavior of a Natural Gas Bubble in a Simulated Deep Sea Environment," *Chem. Eng. Sci.*, **36**, 183 (1981).

Makogon, Y. F., *Hydrates of Hydrocarbons*, Pennwell, Tulsa, OK (1997).

Mochizuki, T., and Y. H. Mori, "Numerical Simulation of Transient Heat and Mass Transfer Controlling the Growth of a Hydrate Film," *Ann. N.Y. Acad. Sci.*, **912**, 642 (2000).
Mori, T., and Y. H. Mori, "Characterization of Gas Hydrate Formation in a Direct-Contact Cool Storage Process," *Int. J. Refrig.*, **12**, 259 (1989a).
Mori, Y. H., and T. Mori, "Formation of Gas Hydrate with CFC Alternative R-134a," *AIChE J.*, **35**, 1227 (1989b).
Mori, Y. H., and T. Mochizuki, "Modeling of Simultaneous Heat and Mass Transfer to/from and Across a Hydrate Film," *Ann. N.Y. Acad. Sci.*, **912**, 633 (2000).
Mullin, J. W., *Crystallization*, 3rd Edition, Reed Educational and Professional Publishing, Oxford (1993).
Nojima, K., and Y. H. Mori, "Clathrate Hydrate Formation on Single Refrigerant Vapor Bubbles Released into Water: An Observational Study," *Proc. Int. Heat Transfer Conf.*, Rugby, UK, Institution of Chemical Engineers, p. 377 (1994).
Ohmura, R., T. Shigetomi, and Y. H. Mori, "Formation, Growth and Dissociation of Clathrate Hydrate Crystals in Liquid Water in Contact with a Hydrophobic Hydrate-Forming Liquid," *J. Cryst. Growth*, **196**, 164 (1999).
Servio, P., "Kinetic, Equilibrium and Morphology Studies of Hydrate Forming Systems," PhD Thesis, Dept. of Chemical and Biological Engineering, Univ. of British Columbia, Vancouver, BC, Canada.
Servio, P., and P. Englezos, "Measurement of the Amount of Dissolved Methane in Water in Equilibrium With its Hydrate," *J. Chem. Eng. Data*, **47**, 87 (2002).
Servio, P., and P. Englezos, "Effect of Temperature and Pressure on the Solubility of Carbon Dioxide in Water in the Presence of Gas Hydrates," *Fluid Phase Equilibria*, **190**, 127 (2001).
Shindo, Y., Y. Fujioka, Y. Yanagisawa, T. Hakuta, and H. Komiyama, "Formation and Stability of CO_2 Hydrate," *Proc. Int. Workshop on Interaction between CO_2 and Ocean*, Tsukuba, Japan, p. 111, [cited by Sugaya and Mori (1996)] (1993).
Sloan, E. D., *Clathrate Hydrates of Natural Gases*, Dekker, New York (1998).
Suess, E., G. Bohrmann, J. Greinert, and E. Lausch, "Flamable Ice," *Sci. Amer.,* **281** (5), 76 (1999).
Sugaya, M., and Y. H. Mori, "Behaviour of Clathrate Hydrate Formation at the Boundary of Liquid Water and a Fluorocarbon in Liquid or Vapor State," *Chem. Eng. Sci.*, **51**, 3505 (1996).
Topham, D. R., "The Formation of Gas Hydrates on Bubbles of Hydrocarbon Gases Rising in Sea Water," *Chem. Eng. Sci.*, **39**, 821 (1984).
Uchida, T., T. Ebinuma, J. Kawabata, and H. Narita, "Microscopic Observations of Formation Processes of Clathrate-Hydrate Films at an Interface between Water and Carbon Dioxide," *J. Crystal Growth*, **204**, 348 (1999).
Uchida, T., T. Ebinuma, and H. Narita, "Observations of CO_2-Hydrate Decomposition and Reformation Process," *J. Cryst. Growth*, **217**, 189 (2000).

Manuscript received March 25, 2002, and revision received June 28, 2002.